JOURNAL OF CHEMICAL INFORMATION AND MODELING

Article

pubs.acs.org/jcim

Application of a FLAP-Consensus Docking Mixed Strategy for the Identification of New Fatty Acid Amide Hydrolase Inhibitors

Giulio Poli, Niccolò Giuntini, Adriano Martinelli, and Tiziano Tuccinardi*

Department of Pharmacy, University of Pisa, 56126 Pisa, Italy

Supporting Information

ABSTRACT: Fatty acid amide hydrolase (FAAH) is the principal responsible for the termination of anandamide signaling, a major actor of the endocannabinoid system. The indirect stimulation of endocannabinoid responses achieved through FAAH inhibition can represent a valid pharmacological strategy for the treatment of neurodegenerative and neuroinflammatory diseases such as multiple sclerosis, Alzheimer's, Huntington's, and Parkinson's diseases, as well as rheumatoid arthritis, gastrointestinal inflammatory states, anxiety, and other pathologies. With the aim of identifying new noncovalent FAAH inhibitors and also experimentally validating the reliability of the recently reported consensus docking approach, we filtered a commercial database of about 1 million compounds by using a mixed FLAP (fingerprints for ligands and proteins) consensus docking approach. Enzymatic assays showed FAAH inhibitory activity and selectivity versus MAGL for 8 out of the 10 top ranked compounds, with IC_{50} values in the low micromolar range for the two most active compounds. These results demonstrate the reliability of the virtual screening strategy and constitute an experimental validation of the consensus docking approach. Moreover, the two most active compounds described could represent promising leads for the development of high potent noncovalent FAAH inhibitors.

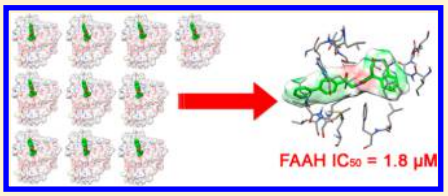

INTRODUCTION

The first mammalian amidase to be cloned was from rat liver plasma membrane, in 1996, and was called FAAH (fatty acid amide hydrolase) due to the plurality of fatty acid amides (FAAs) that the enzyme could accept as substrates.[1] This enzyme is a 63 kDa protein with 579 amino acids belonging to the amidase-signature family, whose members share a common conserved amino acid sequence comprising about 130 residues, the so-called amidase-signature sequence.[2] FAAH shows a nonconventional catalytic mechanism where the unusual hydrolytic triad composed by Lys142, Ser217, and Ser241 interactions through a network of hydrogen bonds that makes proton exchange easier and allows the enzyme to degrade amides and esters with equivalent catalytic efficiencies.[3] The main substrate of FAAH enzyme is anandamide (*N*-arachidonoylethanolamide), which is the first endogenous ligand discovered for the cannabinoid receptor CB_1 and still represents a major actor of the endocannabinoid system.[2] FAAH is mainly responsible for the termination of anandamide signaling through its hydrolysis, in both the central nervous system and in peripheral tissues.[4] Other important FAAH substrates are represented by *N*-oleoylethanolamide, a lipid mediator that limits food intake which has been very recently shown to determine neuroprotection of the nigrostriatal system in experimental parkinsonism by targeting the PPAR-α nuclear receptor;[5] Oleamide, a selective endogenous agonist of CB_1 receptors well-known for its sleep-inducing effect;[6] *N*-palmitoyletanolamide, endowed with a strong anti-inflammatory power due to the activation of PPAR nuclear receptors, and whose levels in the brain are subjected to a 10-fold increase after inactivation of the FAAH gene.[7] The elevation of endogenous levels of FAAs obtained by a genetic or pharmacological inactivation of FAAH produces anti-inflammatory and analgesic as well as antidepressant, anxiolytic, and sleep-inducing phenotypes, which however occur in the absence of alterations in cognition, weight gain, motility, or body temperature usually associated with direct CB_1 agonists. For this reason, FAAH inhibition is an interesting approach to induce the beneficial properties of CB_1 receptor stimulation without unwanted side effects that are observed by using direct agonists.[8] FAAH inhibition is particularly effective at reducing excitotoxic progression in the brain and protecting against synaptic compromise, neuronal death, and the behavioral symptoms of excitotoxic brain damages like stroke and traumatic brain injuries. It has also been proven to protect against excitotoxic hippocampal damage and preserve mechanisms necessary for memory encoding.[9] This indirect stimulation of endocannabinoid responses achieved through FAAH inhibition can represent a valid pharmacological strategy for the therapy of multiple sclerosis as well neurodegenerative and neuroinflammatory diseases such as Alzheimer's, Huntington's, and Parkinson's diseases.[10] FAAH inhibition has been also identified as a promising strategy for the treatment of a broad range of painful and inflammation states, since it produces anti-inflammatory and antihyperalgesic effects in a wide range of animal models, without generating the typical side effects normally showed in consequence of a direct stimulation of cannabinoid receptors.[11] These include osteoarthritis and rheumatoid arthritis as well as gastrointestinal

Received: November 12, 2014
Published: March 6, 2015

DOI: 10.1021/ci5006806
J. Chem. Inf. Model. 2015, 55, 667−675

inflammatory states, particularly those characterized by abdominal pain and motility imbalances like inflammatory bowel diseases and irritable bowel syndrome.[12] Other possible applications of FAAH inhibitors concern the treatment of obesity and diabetes,[12] drug, alcohol, and nicotine addiction,[13] stress-induced anxiety, and stress-related psychopathologies.[14]

Considered the wide range of possible therapeutic strategies which can rely on FAAH inhibition, it is not surprising that the search for novel small molecule FAAH inhibitors is an expanding field of study. A significant number of FAAH inhibitors has already been reported in literature, and most of them belong to the major classes of covalent inhibitors. At present, only a small number of potent FAAH ligands, for which a noncovalent inhibitory profile has been well-characterized, can be found in literature. In 2009 Wang and co-workers reported benzothiazole analogues showing potent and selective FAAH inhibition properties,[15] Gustin and co-workers in 2011 reported a series of pyrrolopyridines derivatives whose unique noncovalent binding mode was unquestionably revealed by X-ray studies,[16] Gowlugari and co-workers recently reported the discovery of the tetrahydropyridopyridine compound RN-450 and finally a series of noncovalent 1-aryl-2-((6-aryl)pyrimidin-4-yl)amino)ethanols with low nanomolar activity toward human FAAH was patented and then published by Janssen Pharmaceutical Companies.[17,18]

Very recently, we have reported an in silico evaluation of the consensus docking approach by applying a consensus cross-docking and by using enriched database.[19] From a qualitative point of view, the results highlighted that consensus docking was able to predict the ligand binding pose better than the single docking whereas, concerning the virtual screening studies, the obtained results suggested that this approach performed as well as the best available methods found in literature. To the best of our knowledge, no experimental validations have been reported in literature for this approach so far. In the present study, with the aim of identifying new FAAH noncovalent inhibitors and also experimentally testing the reliability of the consensus docking approach, we performed a virtual screening (VS) study by using a mixed FLAP (fingerprints for ligands and proteins) consensus docking approach.

MATERIALS AND METHODS

Database Generation. The 18 Maximum Unbiased Validation data sets of decoys[20] were prefiltered by selecting only compounds with a molecular weight between 350 and 550 g/mol. The retained compounds belonging to the different data sets were collected in a unique decoy data set of 43 629 molecules. The same prefilter was applied to both Vitas-M and Enamine databases to create a single database of about 1 million commercial compounds. Both databases were enriched with the six known active noncovalent FAAH inhibitors and processed by FLAP to generate a screening data set. In this procedure a set of conformers is generated for each compound, then GRID molecular interaction fields (MIFs) are calculated for each conformer and translated into the fingerprints on which all FLAP screening calculations are based. The database generation was performed by setting all the parameters as their defaults, with the exception of enabling the removal of duplicates, so as to avoid the inclusion of identical decoy molecules. Conformational analyses were performed through a random search saving a maximum of 25 conformers per ligand and rejecting those with a root-mean-square deviation (RMSD) < 0.3 Å from any other. The GRID probes O (H-bond acceptor), N1 (H-bond donor), DRY (hydrophobic), and H (shape) with a grid resolution of 0.75 Å were used for generating the MIFs.

FLAP Virtual Screening Analyses. *FLAP Ligand-Based Virtual Screening.* Each of the six different ligand-based virtual screenings was performed by using as a template structure one of the six known active reference FAAH ligands. Calculations were ran by leaving all the settings as their defaults, i.e., (a) using only one conformer of the query structure as a template, (b) considering the fingerprint matching, (c) using a low level of accuracy. For the following virtual screening processes, the compound used as a query structure was removed from the set of active molecules.

FLAP Receptor-Based Virtual Screening. The crystal structure of chain A of the humanized variant of rat FAAH (h/rFAAH, PDB code 3OJ8[21]) was used as a template for the receptor-based VS. This crystal structure corresponds to the h/rFAAH complexed with a covalent inhibitor. We selected this structure instead of choosing the two available structures of FAAH complexed with a noncovalent inhibitor (3QK5 and 3QJ9 PDB code[16]) because these last two structures corresponded to rat FAAH and also because a representative ligand of this noncovalent class of compounds was included in the active data set of FAAH inhibitors. The usage of the corresponding FAAH protein could therefore lead to a bias in the receptor-based FLAP screening. The X-ray complex was first subjected to two minimization steps with the software AMBER 11.[22] The complex was set in a rectangular parallelepiped water-box (TIP3P explicit solvent model) and solvated with a 10 Å water cap. Chlorine ions were added as counterions for neutralizing the system. Two steps of minimization were then performed. In the first step the complex was kept fixed with a position restraint of 500 kcal/(mol Å^2), allowing the movement of water molecules. In the second stage the whole system was minimized through 20 000 steps of steepest descent followed by conjugate gradient until a convergence of 0.05 kcal/(mol Å) was reached. All the α carbons of the protein were blocked with a harmonic force constant of 10 kcal/(mol Å^2). The water and chlorine ions were stripped and the bound ligand extracted from the minimized structure. The protein structure was loaded into FLAP and processed by the FLAP default basic filters for PDB files. The automatic identification of the protein cavities was carried out by means of the FLAPsite algorithm,[23] and the bound ligand was loaded to verify its placement into the top-scored pocket, that corresponded to the protein catalytic site and that was employed as the query pocket for the receptor-based VS. The screening was ran by using a max minima point value of 100 to allow FLAP to consider in the calculation all the pharmacophoric hotspots obtained by the condensation of the receptor MIFs. Default values were used for all other parameters.

FLAP Pharmacophore-Based Virtual Screening. The pharmacophore model was built through the FLAPpharm tool implemented in FLAP.[23] The six known active noncovalent FAAH inhibitors that were used for enriching the two databases (see the Database Generation section) were employed as template structures for the alignment, performed by leaving all the settings as their defaults. The FLAPpharm algorithm, rather than extracting features, finding common sets, and then aligning the molecules based on these, works in a reverse way. Ligands are aligned to each other to find the

DOI: 10.1021/ci5006806
J. Chem. Inf. Model. 2015, 55, 667−675

optimal MIF similarity across the set, then subsequently the pharmacophore is extracted. In this way only the model showing the best overlap of the MIFs among the various models generated by the FLAPPharm tool during the alignment process was used. The following pharmacophore-based VS was performed setting all the parameters as their defaults.

Docking Procedures. In all docking analyses compounds were docked in the catalytic site of chain A of the h/rFAAH minimized as reported above. For all the docking analyses only the top scored pose was considered.

AUTODOCK 4.2.3. AUTODOCK Tools utilities[24] were employed for identifying the torsion angles in the compounds, adding the solvent model, and assigning the Gasteiger atomic charges to the protein and ligands. The region of interest used by AUTODOCK was defined by considering the bound ligand as the central group of a grid box of 10 Å in the *x*, *y*, and *z* directions. Energetic map calculations were carried out by employing a grid spacing of 0.375 Å and a distance dependent function of the dielectric constant. By use of the Lamarckian genetic algorithm, the docked ligands were subjected to 20 runs of the AUTODOCK search using 2 500 000 steps of energy evaluation. All other settings were left as their defaults.

DOCK 6.5. The MS software was employed to generate the molecular surface of the binding site,[25] creating the Connolly surface with a probe of 1.4 Å radius. The points of the surface and the vectors normal to it were used by the Sphgen program for building a set of spheres with radii ranging from 1.4 to 4 Å describing the negative image of the site. The spheres within a radius of 10 Å from the bound ligand were employed for the representation of the docking site. The best grid scored within the 500 orientations calculated by DOCK 6.5, for each ligand, was considered. The AM1-BCC method of the Antechamber suite (AMBER 11)[22] was used for calculating the ligand charge.

FRED 3.0. FRED[26] needs a set of conformations for each input molecule. The conformers were created by OMEGA2.[27] Default values were used for all sampling parameters except for the energy window (50.0), the maximum number of conformers (10 000), the time limit (1200), and the RMSD value below which two conformations were considered to be similar (0.3 Å). The binding site region contained all residues which stayed within 10 Å from the bound ligand in the X-ray structure. The FRED docking calculation is divided into two steps: shape-fitting and optimization. During the shape-fitting, a smooth Gaussian potential is employed to place the ligand into the binding site. A series of three optimization filters was then performed, which consisted of refinement of the positions of the ligand's hydroxyl hydrogen atoms, rigid body optimization, and optimization of the ligand pose in the dihedral angle space. In the last optimization step, the Chemgauss3 scoring function was used. After the docking calculation, the poses were scored independently by Chemgauss4.

GLIDE 5.0. The docking site was defined by a cubic box of 10 Å in the *x*, *y*, and *z* directions centered on the bound ligand. The possibility of imposing a limit for the number of atoms a ligand may have in case of being docked was disabled, therefore all the ligands were docked independently from the number of their atoms. All other settings were left as GLIDE[28] defaults. For each ligand two docking analyses were performed using the standard precision (SP) and extra precision (XP) methods.

GOLD 5.1. The docking site was defined as the region comprising all residues which stayed within 10 Å from the bound ligand in the h/rFAAH crystal structure; the "allow early termination" option was disabled, while the possibility for the ligand to flip ring corners was enabled. The GOLD[29] defaults were employed for all other settings, and the ligands were subjected to 30 genetic algorithm runs. Four docking analyses were performed by employing each of the four fitness functions implemented in GOLD, i.e. ChemPLP (PLP), GOLDScore (GS), ASP, and ChemScore (CS).

AUTODOCK VINA 1.1. The input files originated by the AUTODOCK Tools utilities for AUTODOCK calculations, including the grid box dimensions, were used. The exhaustiveness parameter was set to 10 and the Energy_range to 1, whereas the AUTODOCK VINA[30] defaults were used for all other settings.

Consensus Docking Evaluation. Applying the ten docking procedures, ten different binding dispositions (best scored poses) were obtained by docking each ligand into the h/rFAAH binding site. The RMSD of each of these docking poses with respect to the remaining nine was evaluated by considering only the ligand heavy atoms and using the rms_analysis software of the GOLD suite. On this basis, for each ligand docked into the protein binding site a 10 × 10 matrix was generated reporting the RMSD results. By using an in-house program these results were clustered, so that among the ten results all the similar docking poses were clustered together. The complete-linkage method was used as clustering algorithm, which is an agglomerative type of hierarchical clustering. This method starts considering each element is in a cluster of its own. The clusters are then sequentially combined into larger ones until all elements are in the same cluster. At each step, the two clusters separated by the shortest distance are combined. We selected an RMSD threshold of 2.0 Å, therefore the so obtained clusters contained the group of poses which were less than 2.0 Å away from all others poses belonging to the same cluster. As a result, for each ligand subjected to the consensus docking protocol the so-called "consensus level" corresponded to the number of docking procedures whose results could be clustered into a same cluster indicating very similar binding modes. The consensus level was used as a parameter to evaluate the docking results and to filter commercial compounds.

Molecular Dynamic Simulations. All simulations were carried out using AMBER 11.[22] The complexes were placed in a rectangular parallelepiped water-box (TIP3P explicit solvent model) and were solvated with a 10 Å water cap. Chlorine ions were added as counterions. Before running the molecular dynamic (MD) simulations, two steps of minimization were performed following the same procedure described above. Particle mesh Ewald electrostatics and periodic boundary conditions were used in the simulation.[31] The MD trajectories were run using the minimized structures as the starting conformations. The time step of the simulations was 2.0 fs with a cutoff of 10 Å for the nonbonded interaction and SHAKE was used to keep all bonds involving hydrogen atoms rigid. Constant-volume periodic boundary MD was carried out for 300 ps, during which the temperature was raised from 0 to 300 K. Then 1.7 ns of constant pressure periodic boundary MD was performed at 300 K by using the Langevin thermostat to keep the temperature of our system constant. General amber force field (GAFF) parameters were assigned to the ligands, while partial charges were calculated using the AM1-BCC method. The MD trajectories were analyzed by using the Ptraj suite of AMBER 11. The ligand's disposition was monitored, and by using the docking result as a reference pose, and all the ligands

DOI: 10.1021/ci5006806
J. Chem. Inf. Model. 2015, 55, 667−675

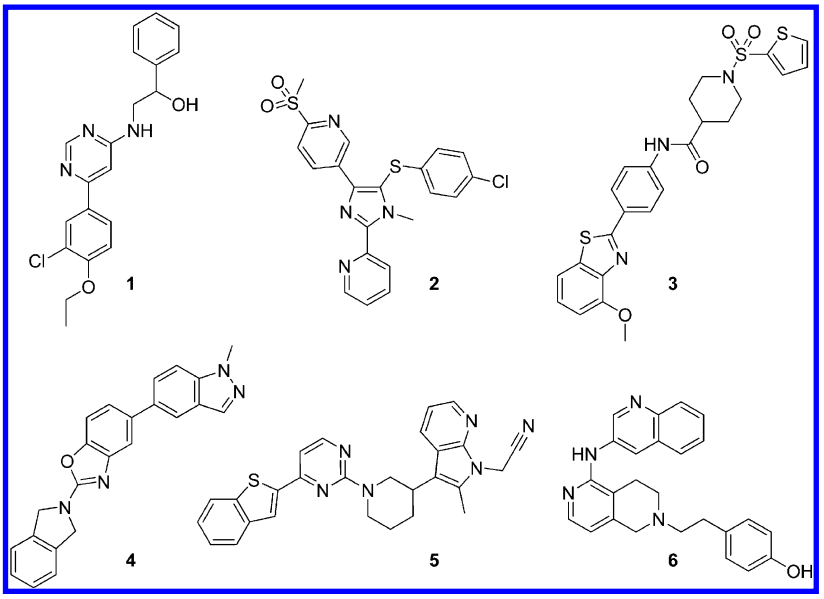

Figure 1. Representative active FAAH inhibitors used in the enriched data set.

that showed an average RMSD greater than 2 Å with respect to the reference disposition were discarded.

Energy Evaluation. We extracted from the last 1.7 ns of MD of the **VS3**− and **VS8**−FAAH MD trajectories, 170 snapshots (at time intervals of 10 ps) for each species (complex, receptor, and ligand). The SANDER module of AMBER 11 was used for calculating van der Waals, electrostatic, and internal energies. Polar energies were calculated with the PBSA module of AMBER 11 (using the Poisson−Boltzman method) using dielectric constants of 1 and 80 to represent the gas and water phases, respectively. The MOLSURF program was used for calculating the nonpolar energies. For the comparison of the ligand−protein energetic interactions, we considered the entropic value as approximately constant.

Virtual Screening Evaluation. The VS results were assessed through the use of the enrichment factor (EF) and the area under curve (AUC) of the receiver operator characteristic (ROC) curve. The EF measures the enrichment of the method compared with random selection:

$$EF = [t_p/(t_p + f_n)](NC_{tot}/NC)$$

where t_p is the number of known active ligands retrieved (true positives); f_n is the number of known active ligands discarded during the VS filtering (false negatives); NC_{tot} is the total number of compounds of the database; NC is the total number of molecules obtained by the VS protocol. The $EF_{1\%}$ and $EF_{10\%}$ indicates the EF values retaining the 1% and 10% of the whole database. The maximum value that can be reach is 100 ($EF_{1\%}$) and 10 ($EF_{10\%}$); therefore, all the evaluated EF results were reported as the percentage of these values. The AUC is the area under the ROC curve; an AUC of 0.5 corresponds to a random discrimination between actives and decoys, whereas an AUC very close to 1.0 corresponds to an ideal case, in which all the known true actives are ranked before all the decoys.

FAAH Inhibition Assay. The IC_{50} values of the selected ligands were obtained in 96-well microtiter plates. The FAAH reaction was carried out at a final volume of 200 μL in 125 mM Tris buffer, pH 9.0, containing 1 mM EDTA. A total of 150 μL of AMC arachidonoyl amide 13.3 μM (final concentration = 10 μM) was added to 10 μL of DMSO containing the suitable amount of ligand. The reaction was started by the addition of 40 μL of FAAH (0.9 μg/well) so that the assay was linear over 30 min. The final concentration of the analyzed compounds varied from 10 to 0.000 01 μM for **CAY10499** and from 200 to 0.0128 μM for the other compounds. After the reaction had proceeded for 30 min, fluorescence values were measured by using a VictorX3 PerkinElmer instrument at an excitation wavelength of 340 nm and an emission of 460 nm. Two reactions were also carried out: one reaction containing no compounds and the second one containing neither inhibitor nor enzyme. IC_{50} values were obtained from experimental data using the sigmoidal dose−response fitting of GraphPad Prism software. A blank analysis was carried out for each compound concentration to remove possible false positive results, and the final fluorescence results were derived subtracting the fluorescence produced by the presence of all the components except FAAH in the same conditions.

FAAH Preincubation Assay. The FAAH reaction was carried out at a final volume of 200 μL in 125 mM Tris buffer, pH 9.0, containing 1 mM EDTA. A total of 150 μL of FAAH (0.9 μg/well) was added to 10 μL of DMSO containing the suitable amount of compound. After 0, 30, and 60 min of incubation time, the reaction was started by adding 40 μL of AMC arachidonoyl amide 50 μM. The enzyme activity was then measured according to the procedure described above.

MAGL Inhibition Assay. Human recombinant MAGL and 4-nitrophenylacetate substrate (4-NPA) were purchased from Cayman Chemical. The MAGL reaction was carried out at a final volume of 200 μL in 10 mM Tris buffer, pH 7.2, containing 1 mM EDTA. A total of 150 μL of 4-NPA 133.3 μM (final concentration = 100 μM) was added to 10 μL of DMSO containing the suitable amount of ligand.[32] The reaction was started by adding 40 μL of MAGL (11 ng/well) so that the assay was linear over 30 min. After the reaction had proceeded for 30 min, absorbance values were measured by using a VictorX3 PerkinElmer instrument at 405 nm. Two reactions were also carried out: one reaction containing no compounds and the second one containing neither inhibitor nor enzyme. A blank analysis was carried out for each compound concentration to remove possible false positive results and the final

DOI: 10.1021/ci5006806
J. Chem. Inf. Model. 2015, 55, 667−675

absorbance results were obtained subtracting the absorbance produced by the presence of all the components except MAGL in the same conditions.

RESULTS AND DISCUSSION

As already reported,[19] the main Achilles' heel of the consensus docking approach is the required computing time. In fact, by using this method a whole data set of molecules should be subjected to all the docking procedures. For this reason, large libraries of compounds require large amount of CPU time. One of the possible solutions of this problem could be the application of a prefilter step able to decrease the number of compounds to be analyzed. Recently we verified the reliability of FLAP software for the VS studies;[33] therefore, we tested the possibility of applying a FLAP prefilter for selecting potential noncovalent FAAH inhibitors.

FLAP Reliability Analysis. An enriched database constituted by FAAH noncovalent inhibitors and decoys was built up. To this aim, ligands for which an FAAH noncovalent inhibition property was reported in the literature were studied and six different classes of compounds were identified as the most promising noncovalent FAAH inhibitors. In 2009 a series of aryl-hydroxyethylamino-pyrimidines[17] (compound **1** of Figure 1) and imidazole derivatives[34] (compound **2**) were patented by Janssen Pharmaceutical Companies and Merck & Co, respectively, as nanomolar noncovalent FAAH inhibitors. In the same year Wang and co-workers reported the synthesis and analysis of novel benzothiazole-based analogues that proved to be potent and selective FAAH inhibitors (compound **3**).[15] Renovis patented in 2010 a wide library of nanomolar FAAH inhibitors characterized by the presence of a central benzoxazolamine scaffold (compound **4**),[35] whereas in 2011 Gustin and co-workers reported the first crystal structure of a noncovalent ligand complexed with FAAH enzyme (compound **5**).[16] Finally in 2012, Gowlugari and co-workers discovered a series of alkylated tetrahydropyridopyridines with promising activity and characterized by a noncovalent interaction with the FAAH enzyme (compound **6**).[36] On the bases of these results a representative compound of each of the six FAAH inhibitor classes was built and included in the enriched database as active molecule (see Figure 1).

As regards the choice of decoys, we downloaded all the decoys included in the Maximum Unbiased Validation data sets reported by Rohrer and Baumann in 2009.[20] We selected all the compounds with a molecular weight between 350 and 550 g/mol that corresponded to the molecular weight possessed by the active molecules included in the data set. The so-obtained enriched database consisted of six active molecules and 43 629 decoys and was then used to assess the ability of the software FLAP (fingerprints for ligands and proteins) in separating FAAH inhibitors from decoys. Ligand-based, receptor-based, and pharmacophore-based VS procedures are implemented in FLAP and they are all based on the comparison of the GRID MIFs and/or the GRID atom type of ligands and proteins, after their translation into fingerprints.[37] To this aim, a FLAP database storing for all compounds the full set of information necessary for the screening process has to be created (see Materials and Methods for details). This FLAP database was screened by using the various available approaches, and the results were assessed in terms of $EF_{1\%}$, $EF_{10\%}$, and AUC. As a first step, the ligand-based VS protocol of FLAP was applied; by using this technique, FLAP compared each template molecule with the whole data set of compounds through the superposition of the MIF-based pharmacophoric features organized in quadruplets. The test compounds were then aligned to the template, based on the best matching quadruplet pairs, and various scores corresponding to the best MIFs overlapping, as well as their combinations, were obtained for each molecule. As shown in Figure 2, the use of compound **1** as a template yielded

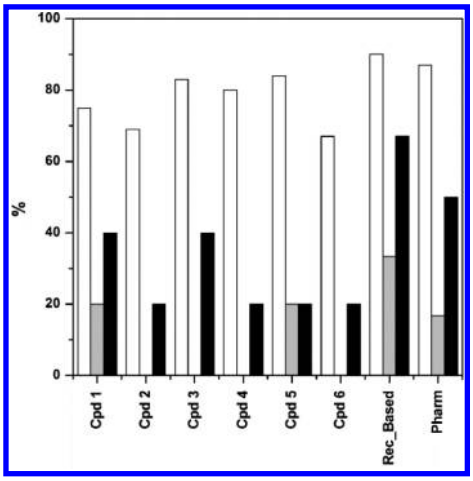

Figure 2. Percentage of AUC (white), $EF_{1\%}$ (gray), and $EF_{10\%}$ (black) values obtained for the enriched data set. Cpdx = ligand-based (Cpdx is the selected template), Rec_Based = receptor-based, and Pharm = pharmacophore-based approach. By using as a template compounds **2**, **3**, and **4**, the $EF_{1\%}$ was zero.

the best results, showing AUC, $EF_{1\%}$, and $EF_{10\%}$ values of 75%, 20%, and 40%, respectively. The pharmacophore and the receptor-based approaches were also evaluated. For the second approach the deposited structure of the humanized variant of rat FAAH (h/rFAAH, PDB code 3OJ8[21]) was energy minimized and used as a template (see the Materials and Methods for details). As shown in Figure 2, the receptor-based VS evaluation was the best method among those tested with AUC, $EF_{1\%}$, and $EF_{10\%}$ values of 90%, 33%, and 67%, respectively.

With the aim of further testing the reliability of the filtering approach the 59 known active FAAH inhibitors reported in Table S1 were added to the enriched database, resulting in a total of 65 known active inhibitors and about 44 000 compounds. The so obtained new data set was then filtered by using the FLAP receptor-based approach and the statistical results proved again the validity of this approach since the results obtained showed AUC, $EF_{1\%}$, and $EF_{10\%}$ values of 86%, 31%, and 63%, respectively (see Figure 3). A further analysis was carried out including in the enriched database 26 known inactive FAAH inhibitors (see Table S2). None of these compounds was ranked in the first 1% of the database and only 27% of them were ranked in the first 10% of the database, thus supporting the reliability of the procedure.

As we included in active data set compound **5**, which has also been crystallized in complex with rFAAH, we superimposed the binding disposition predicted by the FLAP software with respect to that experimentally observed to verify from a qualitative point of view the reliability of the FLAP receptor-based approach. As shown in Figure 4, the software properly predicted the binding disposition of the ligand since there is a complete matching between the experimental and the predicted pose.

DOI: 10.1021/ci5006806
J. Chem. Inf. Model. 2015, 55, 667−675

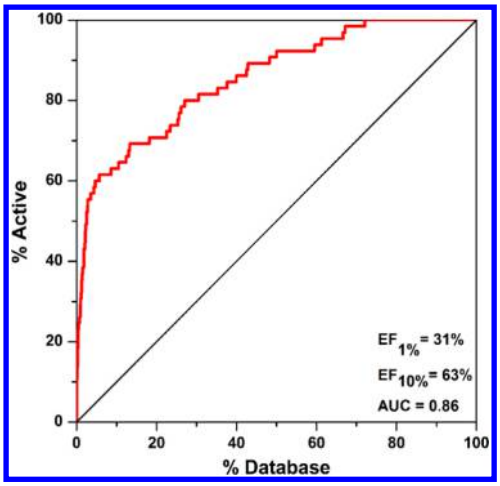

Figure 3. FLAP receptor-based filtering results obtained for the MUV database enriched with the 65 known active FAAH inhibitors.

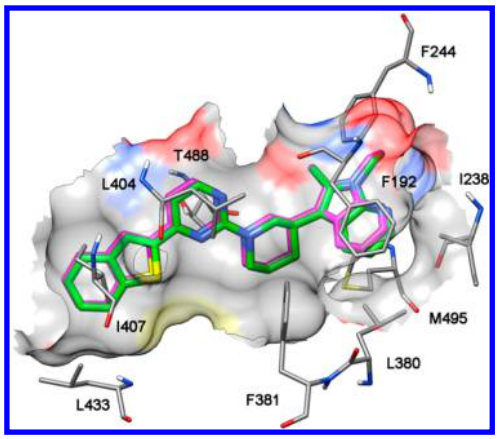

Figure 4. Superimposition between the experimental binding disposition of compound **5** (magenta) and that predicted by the FLAP receptor-based procedure (green).

On the basis of these results, the six known active FAAH ligands were added to the commercial database of about 1 million of compounds (see Material and Methods for details) and the entire data set was then filtered by using the FLAP receptor-based approach. Overall, the results supported the validity of this approach since they were identical to those reached by filtering the MUV database, with AUC, $EF_{1\%}$, and $EF_{10\%}$ values of 90%, 33%, and 67%, respectively. All the commercial ligands having a scoring value better than that resulted for the best scored active compound (i.e., compound **5**) were considered, resulting in 2248 compounds. These compounds, that resulted to be the best scored from the FLAP receptor-based filtering approach, were then subjected to consensus docking studies.

As mentioned above, we have recently reported a consensus docking analysis by applying a consensus cross-docking and by using enriched database.[19] The ten docking procedures already used in that study were applied to the 2248 commercial compounds. For each compound, the obtained ten docking poses (resulted from the calculations carried out by using the ten docking procedures) were clustered together to search for common binding modes (see Materials and Methods for further details). Table 1 shows the consensus docking results: none of the docked compounds showed consensus 10 or 9. However, 2 compounds showed consensus 8, and 15, consensus 7. We also applied the consensus docking approach for the six active FAAH inhibitors and compound **5** was the only one that showed a consensus level of 10. We have previously reported the application of consensus docking for other enriched data sets,[19] and in those studies only an average of about 10% of known active molecules showed a consensus level of 10. Therefore, the results obtained here confirmed this trend, suggesting that the consensus docking protocol has the disadvantage of generating false negatives.

Table 1. Consensus Docking Results for the Filtered Commercial Database

consensus level	number of compounds
10	0
9	0
8	2
7	15
6	47
5	123
4	284
3	694
2	739
1	344

The 17 compounds that showed at least a consensus level of 7 were subjected to a MD simulation to verify the stability of the docking pose. To set up the simulation protocol, the complex between compound **5** and h/rFAAH was used as a test. The protein−ligand complex was subjected to a total of 2 ns of MD simulation; as shown in Figure S1 after about 500 ps the system reached an equilibrium, since the total energy for the last 1.5 ns showed to be roughly constant. By analyzing the RMSD of the ligand's position with respect to the starting structures during the simulation, we observed an average RMSD of 0.6 Å. The 17 compounds that showed at least a consensus level of 7 were subjected to MD simulation by applying the procedure described above and all the compounds that showed an average RMSD value lower than 2 Å were further considered. As a starting binding pose, the results obtained from the GLIDE XP calculations were used, since for all the 17 compounds, GLIDE XP belonged to the docking procedures that successfully contributed to the consensus level. About 40% of the ligands were discarded by using this filter, and the remaining 10 ligands were purchased and tested for their FAAH inhibition properties together with the reference covalent inhibitor **CAY10499**, which was used as a positive control. We used this compound as a control instead of using one of the six active known FAAH inhibitors that were used for the VS study because it is commercially available and also because it is frequently used as a reference compound for evaluating new FAAH and MAGL inhibitors. As shown in Table 2, 8 out of the 10 tested ligands displayed FAAH inhibitory activity, resulting to a hit ratio of 80%. Moreover, compounds **VS3** and **VS8** showed FAAH inhibitory activity in the low micromolar range.

As shown in Figure 5A, compound **VS3** fitted well the long and predominantly hydrophobic cavity constituting FAAH catalytic site, establishing van der Waals contacts with several residues. The biphenylic portion of the ligand interacted with the residues delimiting the binding site surface, i.e. I407, L429, M436, and W531. Particularly, an aromatic CH−π interaction was observed between the ligand disubstituted phenyl ring and W531. The phenyl ring of the benzocycloheptyl moiety

DOI: 10.1021/ci5006806
J. Chem. Inf. Model. 2015, 55, 667−675

Table 2. Structure and Activity of the Compounds Tested

	Structure	FAAH, IC_{50} (μM)	MAGL, IC_{50} (μM)
VS1	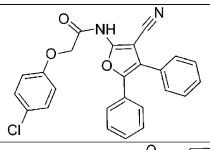	55.3 ± 7.9	> 100
VS2	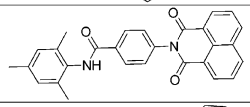	> 100	> 100
VS3	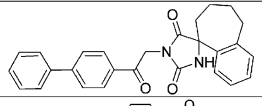	1.8 ± 0.3	> 100
VS4	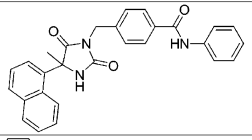	34.6 ± 2.0	97.4 ± 8.2
VS5	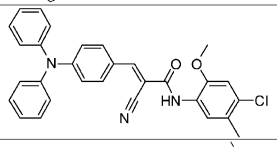	37.9 ± 2.9	> 100
VS6	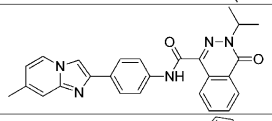	> 100	> 100
VS7	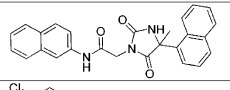	62.3 ± 5.3	18.6 ± 4.2
VS8	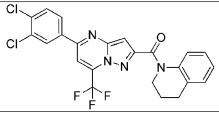	5.3 ± 0.2	> 100
VS9	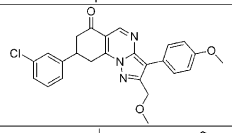	58.6 ± 6.0	> 100
VS10	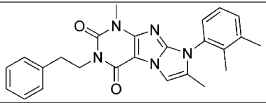	71.9 ± 5.2	> 100
CAY10499	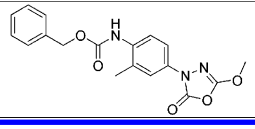	0.013 ± 0.003	0.141 ± 0.020

interacted into a small hydrophobic pocket delimited by F192, I238, L380, and F381, whereas the aliphatic ring took contact with V491 and M495. With its central portion, **VS3** interacted with F381, L404, and T488. Interestingly, the ligand formed a hydrogen bond with the side chain of T488 through its carbonyl oxygen, which was maintained for 90% of the whole MD simulation. On the contrary, **VS8** did not form any hydrogen bond with the protein, only establishing hydrophobic interactions (Figure 5B). Anyway, its activity could be explained by its better fitting into the protein binding site in terms of shape complementarity, filling a wider portion of the receptor excluded volume. The tetrahydropyridine ring of the tetrahydroquinoline moiety of the ligand took closer contacts with V491 and M495, whereas the phenyl ring portion was placed in the small hydrophobic pocket defined by F192, I238, L380, and F381 and showed a $\pi-\pi$ stacking interaction with

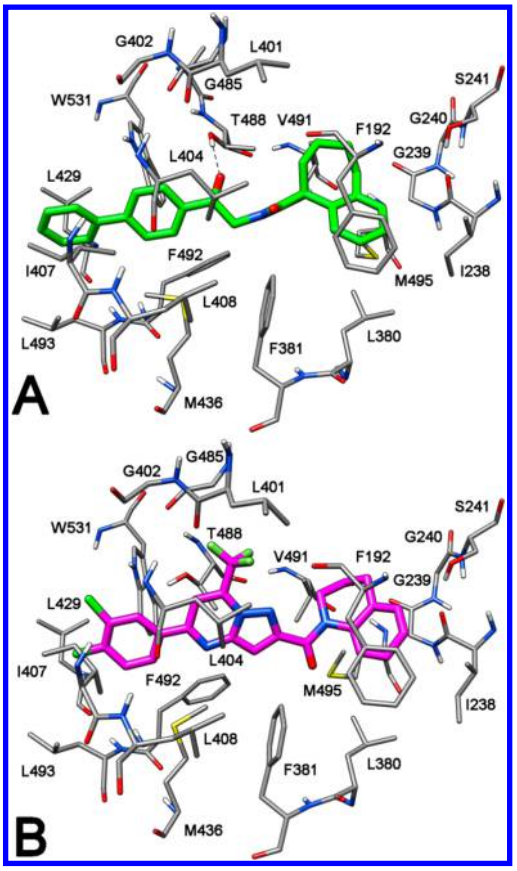

Figure 5. Minimized average structures of compounds **VS3** (A) and **VS8** (B) docked into FAAH.

F192. The 3,4-dichlorophenyl ring interacted with I407, L429, and, particularly, W531, forming an aromatic CH$-\pi$ interaction as observed for **VS3**. Finally, the central pyrazolopyrimidine core took contact with F381, L404, M436, and T488.

The two MD trajectories were further analyzed through the Molecular Mechanics-Poisson–Boltzmann Surface Area (MM-PBSA) method[38] that has been shown to accurately estimate the ligand–receptor energy interaction.[39,40] This approach averages the contributions of gas phase energies, solvation free energies, and solute entropies calculated for snapshots of the complex molecule as well as the unbound components, extracted from MD trajectories, according to the procedure fully described in Materials and Methods. As shown in Table 3,

Table 3. MM-PBSA Results for the VS3– and VS8–FAAH Complexes[a]

	Ele	vdW	PBsur	PB	ΔPBSA
VS3	−4.4	−58.3	−4.7	40.7	−26.7
VS8	−0.3	−62.5	−4.6	39.1	−28.3

[a]ΔPBSA is the sum of the electrostatic (Ele), van der Waals (vdW), polar (PB), and non-polar (PBSur) solvation free energy. Data are expressed as kilocalories per mole.

from this analysis came out that the two compounds showed a similar binding interaction energy (ΔPBSA = −26.7 kcal/mol for **VS3** and ΔPBSA = −28.3 kcal/mol for **VS8**); furthermore, compound **VS3** showed an important electrostatic contribution that was almost zero for **VS8**. However, for compound **VS8**, the van der Waals contribution was about 4 kcal/mol higher than

DOI: 10.1021/ci5006806
J. Chem. Inf. Model. 2015, 55, 667–675

Table 4. IC_{50} (μM) Values of FAAH Inhibitors at Different Preincubation Times

	preincubation time with human FAAH		
compd	0	30 min	60 min
CAY10499	0.0141 ± 0.0021	0.0038 ± 0.0005	0.00018 ± 0.0003
VS3	1.6 ± 0.2	1.2 ± 0.3	1.7 ± 0.2
VS8	5.1 ± 0.3	4.7 ± 0.1	5.0 ± 0.2

that reported for **VS3**, in agreement with the lipophilic interactions showed by this compound.

All the compounds were also tested to measure their activity toward monoacylglycerol lipase (MAGL) and all the compounds resulted to be inactive, with the exception of compound **VS4** and **VS7** that showed an IC_{50} value of 97.4 and 18.4 μM, respectively. Furthermore, different preincubation times of the two most promising inhibitors (i.e., **VS3** and **VS8**) and the FAAH enzyme were tested to evaluate the reversible character of inhibition. In principle, an irreversible inhibitor will increase its ability to block the enzyme with increasingly longer incubation times in the presence of enzyme prior to addition of substrate; on the contrary, a constant IC_{50} supports a reversible mechanism. As expected, the reference compound **CAY10499** showed a time-dependent increase of potency, consistently with its irreversible binding mechanism.[41] On the contrary, no significant increase in their inhibitory potency toward FAAH was shown by compounds **VS3** and **VS8** after 30 and 60 min of preincubation, thus supporting the hypothesis of their reversible inhibition mechanism (see Table 4).

CONCLUSIONS

In this work we performed a VS study by using a mixed FLAP-consensus docking method with the aim of identifying new noncovalent FAAH inhibitors and also experimentally validating the reliability of the consensus docking approach. After testing the ability of the software FLAP with an enriched database, we applied the best procedure to prefilter a database of about 1 million commercial compounds, thus selecting a suitable set of molecules to be subjected to the consensus docking analysis, which was followed by a MD simulation study aimed at verifying the stability of the docking pose for the top ranked molecules. The ten most promising compounds were purchased and tested for their inhibition activity toward FAAH. Eight out of the ten tested compounds showed FAAH inhibition activity, resulting to a hit ratio of 80%. Furthermore, the two most active compounds showed low micromolar IC_{50} values toward FAAH, selectivity against MAGL, and reversible character of inhibition. These results suggest that the optimized procedure developed may be useful to identify novel non-covalent FAAH inhibitors, encouraging us to apply this protocol for other commercial databases. Moreover, the two most active tested compounds could already be considered as leads for the development of novel noncovalent FAAH inhibitors. On the basis of results reported here and previous studies on enriched databases,[19] it can be assumed that the consensus docking approach can be profitably applied also for other targets and not only for identifying new FAAH inhibitors. However, further experimental validations on other targets are needed to support this hypothesis.

ASSOCIATED CONTENT

Supporting Information

Analysis of the MD simulation of compound **5** complexed with h/rFAAH, tables reporting the known active and inactive FAAH inhibitors used in the study. This material is available free of charge via the Internet at http://pubs.acs.org.

AUTHOR INFORMATION

Corresponding Author

*E-mail: tiziano.tuccinardi@farm.unipi.it. Phone: +39 0502219595.

Notes

The authors declare no competing financial interest.

ACKNOWLEDGMENTS

Financial support for this project was provided by the Italian Ministero dell'Università e della Ricerca (MIUR), under the National Interest Research Projects framework (PRIN_2010_5YY2HL). Many thanks are due to Prof. Maurizio Botta for the use of the GLIDE program in his computational laboratory (University of Siena, Italy).

REFERENCES

(1) Deutsch, D. G.; Ueda, N.; Yamamoto, S. The Fatty Acid Amide Hydrolase (FAAH). *Prostaglandins, Leukotrienes Essent. Fatty Acids* **2002**, *66*, 201−210.

(2) Labar, G.; Michaux, C. Fatty Acid Amide Hydrolase: From Characterization to Therapeutics. *Chem. Biodiversity* **2007**, *4*, 1882−1902.

(3) Seierstad, M.; Breitenbucher, J. G. Discovery and Development of Fatty Acid Amide Hydrolase (FAAH) Inhibitors. *J. Med. Chem.* **2008**, *51*, 7327−7343.

(4) Cravatt, B. F.; Demarest, K.; Patricelli, M. P.; Bracey, M. H.; Giang, D. K.; Martin, B. R.; Lichtman, A. H. Supersensitivity to Anandamide and Enhanced Endogenous Cannabinoid Signaling in Mice Lacking Fatty Acid Amide Hydrolase. *Proc. Natl. Acad. Sci. U. S. A.* **2001**, *98*, 9371−9376.

(5) Fu, J.; Astarita, G.; Gaetani, S.; Kim, J.; Cravatt, B. F.; Mackie, K.; Piomelli, D. Food Intake Regulates Oleoylethanolamide Formation and Degradation in the Proximal Small Intestine. *J. Biol. Chem.* **2007**, *282*, 1518−1528.

(6) Leggett, J. D.; Aspley, S.; Beckett, S. R.; D'Antona, A. M.; Kendall, D. A. Oleamide is a Selective Endogenous Agonist of Rat and Human CB1 Cannabinoid Receptors. *Br. J. Pharmacol.* **2004**, *141*, 253−262.

(7) Cravatt, B. F.; Saghatelian, A.; Hawkins, E. G.; Clement, A. B.; Bracey, M. H.; Lichtman, A. H. Functional Disassociation of the Central and Peripheral Fatty Acid Amide Signaling Systems. *Proc. Natl. Acad. Sci. U. S. A.* **2004**, *101*, 10821−10826.

(8) Ahn, K.; Johnson, D. S.; Cravatt, B. F. Fatty Acid Amide Hydrolase as a Potential Therapeutic Target for the Treatment of Pain and CNS Disorders. *Expert Opin. Drug Discovery* **2009**, *4*, 763−784.

(9) Karanian, D. A.; Brown, Q. B.; Makriyannis, A.; Kosten, T. A.; Bahr, B. A. Dual Modulation of Endocannabinoid Transport and Fatty Acid Amide Hydrolase Protects Against Excitotoxicity. *J. Neurosci.* **2005**, *25*, 7813−7820.

(10) Micale, V.; Mazzola, C.; Drago, F. Endocannabinoids and Neurodegenerative Diseases. *Pharmacol. Res.* **2007**, *56*, 382−392.

(11) Schlosburg, J. E.; Kinsey, S. G.; Lichtman, A. H. Targeting Fatty Acid Amide Hydrolase (FAAH) to Treat Pain and Inflammation. *AAPS J.* **2009**, *11*, 39−44.

DOI: 10.1021/ci5006806
J. Chem. Inf. Model. 2015, 55, 667−675

(12) Salaga, M.; Sobczak, M.; Fichna, J. Inhibition of Fatty Acid Amide Hydrolase (FAAH) as a Novel Therapeutic Strategy in the Treatment of Pain and Inflammatory Diseases in the Gastrointestinal Tract. *Eur. J. Pharm. Sci.* **2014**, *52*, 173−179.
(13) Panlilio, L. V.; Justinova, Z.; Goldberg, S. R. Inhibition of FAAH and Activation of PPAR: New Approaches to the Treatment of Cognitive Dysfunction and Drug Addiction. *Pharmacol. Ther.* **2013**, *138*, 84−102.
(14) Gunduz-Cinar, O.; Hill, M. N.; McEwen, B. S.; Holmes, A. Amygdala FAAH and Anandamide: Mediating Protection and Recovery From Stress. *Trends Pharmacol. Sci.* **2013**, *34*, 637−644.
(15) Wang, X.; Sarris, K.; Kage, K.; Zhang, D.; Brown, S. P.; Kolasa, T.; Surowy, C.; El Kouhen, O. F.; Muchmore, S. W.; Brioni, J. D.; Stewart, A. O. Synthesis and Evaluation of Benzothiazole-based Analogues as Novel, Potent, and Selective Fatty Acid Amide Hydrolase Inhibitors. *J. Med. Chem.* **2009**, *52*, 170−180.
(16) Gustin, D. J.; Ma, Z.; Min, X.; Li, Y.; Hedberg, C.; Guimaraes, C.; Porter, A. C.; Lindstrom, M.; Lester-Zeiner, D.; Xu, G.; Carlson, T. J.; Xiao, S.; Meleza, C.; Connors, R.; Wang, Z.; Kayser, F. Identification of Potent, Noncovalent Fatty Acid Amide Hydrolase (FAAH) Inhibitors. *Bioorg. Med. Chem. Lett.* **2011**, *21*, 2492−2496.
(17) Apodaca, R.; Breitenbucher, J. G.; Chambers, A. L.; Deng, X.; Hawryluk, N. A.; Keith, J. M.; Mani, N. S.; Merit, J. E.; Pierce, J. M.; Seierstad, M. Aryl-hydroxyethylamino-pyrimidines and Triazines as Modulators of Fatty Acid Amide Hydrolase. WO2009105220, Aug 27, 2009.
(18) Keith, J. M.; Hawryluk, N.; Apodaca, R. L.; Chambers, A.; Pierce, J. M.; Seierstad, M.; Palmer, J. A.; Webb, M.; Karbarz, M. J.; Scott, B. P.; Wilson, S. J.; Luo, L.; Wennerholm, M. L.; Chang, L.; Rizzolio, M.; Chaplan, S. R.; Breitenbucher, J. G. 1-Aryl-2-((6-aryl)pyrimidin-4-yl)amino)ethanols as Competitive Inhibitors of Fatty Acid Amide Hydrolase. *Bioorg. Med. Chem. Lett.* **2014**, *24*, 1280−1284.
(19) Tuccinardi, T.; Poli, G.; Romboli, V.; Giordano, A.; Martinelli, A. Extensive Consensus Docking Evaluation for Ligand Pose Prediction and Virtual Screening Studies. *J. Chem. Inf. Model.* **2014**, *54*, 2980−2986.
(20) Rohrer, S. G.; Baumann, K. Maximum Unbiased Validation (MUV) Data Sets for Virtual Screening Based on PubChem Bioactivity Data. *J. Chem. Inf. Model.* **2009**, *49*, 169−184.
(21) Ezzili, C.; Mileni, M.; McGlinchey, N.; Long, J. Z.; Kinsey, S. G.; Hochstatter, D. G.; Stevens, R. C.; Lichtman, A. H.; Cravatt, B. F.; Bilsky, E. J.; Boger, D. L. Reversible Competitive Alpha-ketoheterocycle Inhibitors of Fatty Acid Amide Hydrolase Containing Additional Conformational Constraints in the Acyl Side Chain: Orally Active, Long-acting Analgesics. *J. Med. Chem.* **2011**, *54*, 2805−2822.
(22) Case, D. A.; Darden, T. A.; Cheatham, T. E.; Simmerling, C. L.; Wang, J.; Duke, R. E.; Luo, R.; Walker, R. C.; Zhang, W.; Merz, K. M.; Roberts, B.; Wang, B.; Hayik, S.; Roitberg, A.; Seabra, G.; Kolossváry, I.; Wong, K. F.; Paesani, F.; Vanicek, J.; Liu, J.; Wu, X.; Brozell, S. R.; Steinbrecher, T.; Gohlke, H.; Cai, Q.; Ye, X.; Wang, J.; Hsieh, M.-J.; Cui, G.; Roe, D. R.; Mathews, D. H.; Seetin, M. G.; Sagui, C.; Babin, V.; Luchko, T.; Gusarov, S.; Kovalenko, A.; Kollman, P. A. *AMBER*, version 11; University of California: San Francisco, CA, 2010.
(23) Sirci, F.; Goracci, L.; Rodriguez, D.; van Muijlwijk-Koezen, J.; Gutierrez-de-Teran, H.; Mannhold, R. Ligand-, Structure- and Pharmacophore-based Molecular Fingerprints: a Case Study on Adenosine A(1), A (2A), A (2B), and A (3) Receptor Antagonists. *J. Comput.-Aided Mol. Des.* **2012**, *26*, 1247−1266.
(24) Morris, G. M.; Huey, R.; Lindstrom, W.; Sanner, M. F.; Belew, R. K.; Goodsell, D. S.; Olson, A. J. AutoDock4 and AutoDockTools4: Automated Docking With Selective Receptor Flexibility. *J. Comput. Chem.* **2009**, *30*, 2785−2791.
(25) *DOCK*, version 6.5; Molecular Design Institute: University of California: San Francisco, CA, 1998.
(26) *FRED*, version 3.0.0; OpenEye Scientific Software: Santa Fe, NM, USA, 2013.
(27) *OMEGA*, version 2.4.6; OpenEye Scientific Software: Santa Fe, NM, USA, 2013.
(28) *GLIDE*, version 5.0; Schrödinger Inc: Portland, OR, 2009.
(29) Verdonk, M. L.; Cole, J. C.; Hartshorn, M. J.; Murray, C. W.; Taylor, R. D. Improved Protein-ligand Docking Using GOLD. *Proteins* **2003**, *52*, 609−623.
(30) Trott, O.; Olson, A. J. AutoDock Vina: Improving the Speed and Accuracy of Docking With a New Scoring Function, Efficient Optimization, and Multithreading. *J. Comput. Chem.* **2010**, *31*, 455−461.
(31) York, D. M.; Darden, T. A.; Pedersen, L. G. The Effect of Long-Range Electrostatic Interactions in Simulations of Macromolecular Crystals - a Comparison of the Ewald and Truncated List Methods. *J. Chem. Phys.* **1993**, *99*, 8345−8348.
(32) Tuccinardi, T.; Granchi, C.; Rizzolio, F.; Caligiuri, I.; Battistello, V.; Toffoli, G.; Minutolo, F.; Macchia, M.; Martinelli, A. Identification and Characterization of a New Reversible MAGL Inhibitor. *Bioorg. Med. Chem.* **2014**, *22*, 3285−3291.
(33) Poli, G.; Tuccinardi, T.; Rizzolio, F.; Caligiuri, I.; Botta, L.; Granchi, C.; Ortore, G.; Minutolo, F.; Schenone, S.; Martinelli, A. Identification of New Fyn Kinase Inhibitors Using a FLAP-based Approach. *J. Chem. Inf. Model.* **2013**, *53*, 2538−2547.
(34) Lin, L. S.; Chioda, M. D.; Liu, P.; Nargund, R. P. Imidazole Derivatives Useful as Inhibitors of FAAH. WO2009152025, Dec 17, 2009.
(35) Kaub, C.; Gowlugari, S.; Kincaid, J.; Johnson, R. J.; O'mahony, D. J. R.; De Los Angeles Estiarte-Martinez, M.; Duncton, M. Compounds Useful as FAAH Modulators. WO2010039186, Apr 8, 2010.
(36) Gowlugari, S.; DeFalco, J.; Nguyen, M. T.; Kaub, C.; Chi, C.; Duncton, M. A. J.; Emerling, D. E.; Kelly, M. G.; Kincaid, J.; Vincent, F. Discovery of Potent, Non-carbonyl Inhibitors of Fatty Acid Amide Hydrolase (FAAH). *MedChemComm* **2012**, *3*, 1258−1263.
(37) Baroni, M.; Cruciani, G.; Sciabola, S.; Perruccio, F.; Mason, J. S. A Common Reference Framework for Analyzing/Comparing Proteins and Ligands. Fingerprints for Ligands and Proteins (FLAP): Theory and Application. *J. Chem. Inf. Model.* **2007**, *47*, 279−294.
(38) Kollman, P. A.; Massova, I.; Reyes, C.; Kuhn, B.; Huo, S.; Chong, L.; Lee, M.; Lee, T.; Duan, Y.; Wang, W.; Donini, O.; Cieplak, P.; Srinivasan, J.; Case, D. A.; Cheatham, T. E. Calculating Structures and Free Energies of Complex Molecules: Combining Molecular Mechanics and Continuum Models. *Acc. Chem. Res.* **2000**, *33*, 889−897.
(39) Tuccinardi, T.; Manetti, F.; Schenone, S.; Martinelli, A.; Botta, M. Construction and validation of a RET TK Catalytic Domain by Homology Modeling. *J. Chem. Inf. Model.* **2007**, *47*, 644−655.
(40) Tuccinardi, T.; Granchi, C.; Iegre, J.; Paterni, I.; Bertini, S.; Macchia, M.; Martinelli, A.; Qian, Y.; Chen, X.; Minutolo, F. Oxime-based Inhibitors of Glucose Transporter 1 Displaying Antiproliferative Effects in Cancer Cells. *Bioorg. Med. Chem. Lett.* **2013**, *23*, 6923−6927.
(41) Muccioli, G. G.; Labar, G.; Lambert, D. M. CAY10499, a Novel Monoglyceride Lipase Inhibitor Evidenced by an Expeditious MGL Assay. *ChemBioChem* **2008**, *9*, 2704−2710.

DOI: 10.1021/ci5006806
J. Chem. Inf. Model. 2015, 55, 667−675